Indian Journal of Chemical Technology
Vol. 32, May 2025, pp. 367-376
DOI: 10.56042/ijct.v32i3.11148

Green one-pot synthesis of cerium oxide nanoparticles utilising *Colocasia esculenta* stalk extract: An approach to antibacterial activities

Nurul Natasha Wazir[1], Siti Nur Syazwani Maadon[1], Nik Rozlin Nik Masdek[3], Mohd Rafii Yusop[4], Nor Hazlina Mat Sa'at[5], Nor'Aishah Hasan[1]* & Nor Monica Ahmad[2]*

[1]School of Biology, Faculty of Applied Sciences, Universiti Teknologi MARA, Cawangan Negeri Sembilan, Kampus Kuala Pilah, 72000 Kuala Pilah, Malaysia

[2]School of Chemistry and Environment, Faculty of Applied Sciences, Universiti Teknologi MARA, Cawangan Negeri Sembilan, Kampus Kuala Pilah, 72000 Kuala Pilah, Malaysia

[3] School of Mechanical Engineering, College of Engineering, Universiti Teknologi MARA, 40450 Shah Alam, Selangor, Malaysia

[4]Institute of Tropical Agriculture and Food Security, Universiti Putra Malaysia (UPM), Serdang, Selangor, Malaysia

[5]Horticulture Research Centre, Malaysian Agricultural Research and Development Institute, Persiaran MARDI-UPM 43400 Serdang, Selangor, Malaysia

*E-mail: normonica@uitm.edu.my (NMA); aishahnh@uitm.edu.my (NAH)

Received 15 May 2024; accepted 19 March 2025

Cerium oxide (CeO_2) nanoparticles have been synthesised (NPs) via the sol-gel method. *Colocasia esculenta* (*C. esculenta*) stalk extract is employed as a green reducing and capping agent during the production. The different precursor concentrations (0.06–0.30 mol/L) are examined to prepare the NPs which exhibited an absorption band at 216 nm. Using X-ray diffraction technique, the average crystallite size of synthesised CeO_2 is found to be 6.44 nm. Transmission electron microscopy images revealed that the NPs are nearly spherical. High-intensity peaks corresponding to cerium (Ce) and oxygen (O) during energy dispersive X-ray spectroscopy assessments, confirm CeO_2 NPs production. The Fourier-transform infrared evaluations also indicated Ce-O stretching and the absence of O-N-O bending in the NPs. Furthermore, the findings demonstrated that the synthesised CeO_2 NPs exhibited susceptibility against all bacteria, except *Bacillus subtilis*.

Keywords: Antibacterial, Cerium oxide nanoparticles, Green synthesis, Stalk extract

Introduction

Research on metal oxide NPs are raising, attributable to its impressive characteristics and wide potential applications. Cerium oxide (CeO_2) is a semiconductor material with a significant energy band gap (3.19 eV) and wavelength range (330–370 nm). The material is also chemically and thermally stable[1–3].

Several researchers synthesised CeO_2 NPs through chemical approaches. For example, Kusuma *et al.*[4] synthesised CeO_2 NPs with average particle size in the range 35–38 nm via sonochemical method. Those NPs were an excellent photocatalyst for wastewater treatment. Similarly, Ramachandrann *et al.*[5] reported the chemical precipitation method for synthesis of CeO_2 NPs using polyvinyl pyrrolidone as an effective capping agent. The NPs were between 19 nm and 33 nm when synthesised at pH 9 to 11. In another study, Trenque *et al.*[6] reported the synthesis of CeO_2 NPs through pulsed laser ablation, photochemical, and hydrothermal approaches. Novel nano-octahedra, nanocubes, or nanorods of CeO_2 NPs were synthesised. Moreover, the particles exhibited superior paraoxon degrading activities.

The effectiveness of physical and chemical techniques in producing reasonable NPs yields is hindered by their harmful precursors and notable costs and energy requirements[7,8]. Consequently, biological or green nanomaterial synthesis procedures are gaining attention. The approaches are more cost-effective, sustainable, biocompatible, reliable, and economical than their physical and chemical counterparts. Furthermore, green synthesis techniques utilising plant extracts offer practicality, ease of handling, and cost-effectiveness without necessitating toxic substances, thus potential alternatives to conventional procedures[9,10].

Phytochemical-rich plant extracts could stabilise NPs during synthesis, resulting in particles with

desirable morphology and size. Plant extracts are capable of substituting chemicals and can be employed as reducing and capping agents in regulating particle formation and preventing aggregation, contributing to the stabilisation of the NPs[11,12]. The effectiveness of plant extracts as reducing and capping agents is attributable to their significant potent phytochemical contents, such as ketones, aldehydes, flavones, amides, terpenoids, carboxylic acids, phenols, and ascorbic acids[13,14].

Several studies reported employing leaf extracts from *Gloriosa superba* (glory lily)[15], *Acalypha indica* (Indian copperleaf)[16], *Aloe vera*[17], *Prosofisjulifora* Mesquite[18], and *Olei europaea* olive[19] for synthesis of NPs. The flower extract from *Hibiscus sabdarifa* Roselle[20] and leaf and flower extracts from *Calotropis procera* giant milkweed[21] were also documented. Successful productions of nano-sized CeO_2 were also attributed to the presence of phytochemicals in the plant extracts. The compounds contain hydroxyl (OH) molecules that facilitate metal ion reductions and further regulate particle growth by capping the surfaces of the nanostructures[1].

Green CeO_2 NPs offer size and shape versatility, contributing to their adaptability for varying applications. The variations stem from several factors, such as reaction temperature and duration, solution pH, Ce salt precursor type, and phytochemical and other component concentrations extracted from the plant. Nevertheless, reports on CeO_2 NPs synthesis with *Colocasia esculenta* (*C. esculenta*) extract stalks are scarce.

C. esculenta or taro is rich in various phytochemicals, including flavonoids, alkaloids, and saponins[22]. The current study also adopted a simple one-pot procedure at different concentrations of the precursor. The optical properties of the NPs synthesised were determined with ultraviolet-visible (UV-Vis) spectroscopy. Furthermore, comprehensive evaluations of purity, structure, and morphology were conducted with X-ray diffraction (XRD), transmission electron microscopy (TEM), Fourier transform infrared spectroscopy (FTIR), scanning electron microscopy (SEM), and energy dispersive X-ray (EDX). The antibacterial properties of the CeO_2 NPs were also assessed against gram-negative and gram-positive bacteria. The findings could offer valuable insights into the potential applications of the nanomaterial in combating microbial infections effectively.

Experimental Section

Materials

The fresh and healthy *C. esculenta* cv Wangi stalks utilised in this study were harvested from the Malaysian Agricultural Research and Development Institute (MARDI), Serdang, Malaysia at 2°59'02.2"N 101°42'09. 97% ethanol and dimethyl sulfoxide (DMSO) were purchased from Merck, while the cerium nitrate hexahydrate ($Ce(NO_3)_3.6H_2O$) and acetone were purchased from Sigma-Aldrich.

Gram-positive [*Staphylococcus aureus* (*S.aureus*) and *Bacillus subtilis* (*B. subtilis*)] and Gram-negative [*Klebsiella pneumonia* (*K. pneumoniae*) and *Escherichia coli* (*E.coli*)] bacteria samples were obtained from the Culture Bank in Laboratory of Microbiology, Universiti Teknologi MARA Cawangan Negeri Sembilan, Kampus Kuala Pilah. The bacteria strains were cultivated in a Thermo Scientific™ Oxoid™ Mueller Hinton broth. All glasswares used were washed with acid followed by distilled water. Deionised (DI) water was also employed throughout the synthesis process.

Stalk extract preparation

The present study adopted the extraction procedures outlined by Mondal *et al.*[23]. Firstly, the taro stalks were incised into small pieces and rinsed thrice with tap water then deionised water to remove impurities. The stalk samples were oven-dried at 80°C to remove water. Subsequently, an electric grinder was employed to ground the dried stalk into fine powder. A total of 10 g of the leaf stalk powder was transferred to a 250 mL beaker containing 100 mL distilled before being boiled at 80°C for 30 min. The dark brown *C. esculenta* leaf stalk extract solution was cooled to room temperature and filtered with Whatman filter paper. The solution was kept in a cleaned Schott bottle at 4°C before use.

Synthesis of CeO_2-NPs with *C.esculenta* stalk extract

The green and simple CeO_2 NPs synthesis approach employed in this study was based on the procedures proposed by Alam *et al.*[24] with minor modifications. Initially, 100 mL of the *C. esculenta* stalk extract was mixed with 0.03 M of $Ce(NO_3)_3 \cdot 6H_2O$. The mixture was constantly agitated for 5 h at 80°C to initiate colloidal solution formation. Further continuous stirring for 30 min led to a thick yellowish-brown gel development. The mixture was left at room temperature for 2 h upon completion of

the reaction. Subsequently, the mixture was subjected to centrifugation at 3000 rpm for 2 min with ethanol and distilled water to eliminate undesired residue. Our team previously published this method[25]; however, optimisation variables were not explored. In this study, we focus on optimising the precursor concentration to investigate its influence on the characteristics of CeO_2 NPs.

The gel was transferred to a glass Petri dish and oven-dried at 80°C overnight to ensure thorough removal of moisture. The dried precipitates were then calcined at 600°C for 2 h to enhance the crystallinity of the CeO_2 NPs yield. The yellow powder was stored in glass vials before being characterised and applied against the bacterial samples. Fig. 1 illustrates the schematic diagram of the CeO_2 NPs synthesis with the *C. esculenta* stalk extract.

Characterisation of CeO_2 NPs

The green synthesised CeO_2 NPs obtained in this study were subjected to several characterisation techniques to determine its optical properties, purity, morphology, and elemental contents. The UV–Vis spectra of CeO_2 NPs were recorded with a T80+ ultraviolet-visible (UV-Vis) spectrophotometer (PG Instruments) within the 200–400 nm range. The XRD analysis of the NPs manufactured in this study was performed using a Rigaku diffractometer. The FTIR spectra within the 500–4000 cm^{-1} spectral range (Perkin Elmer) were used to determine the functional groups in the NPs from employing the stalk extract as the capping and reducing agents. Morphological properties and elemental compositions of the NPs were also examined with SEM and EDX (A Hitachi TM3030 PLUS model), respectively. Further morphological assessment was conducted with TEM (Talos L120C).

Antibacterial assay

The effectiveness of the green CeO_2 NPs in inhibiting bacteria was assessed qualitatively according to the method described by Dar *et al.*[26]. An array of bacterial strains encompassing Gram-positive (*S. aureus* and *B. subtilis*) and Gram-negative species (*E. coli* and *K. pneumoniae*) were selected during the antibacterial activities evaluation. Fresh overnight 100 µL of inoculum from each bacterial sample culture was spread onto Muller Hinton agar plates. Sterile paper discs of 5 mm diameter were precisely positioned in each plate. The discs contained varying concentrations of the CeO_2 NPs (50, 100, 150, 200, and 250 µg/mL). In this study, gentamycin (10 µg) was employed as the positive control, while sterile distilled water served as the negative control. Subsequently, the plates were placed in an incubator for 18–24 h at 37±2°C. The plates were then inspected for inhibition zones around the wells. Each screening assessment was performed in triplicates.

Statistical analysis

The inhibitory zone widths and concentration values recorded in the current study were analysed with the Statistical Packages for Social Science (SPSS) software version 17 for Windows, in accordance with CLSI requirements. The results were reflected in terms of mean and standard deviation. Kruskal-Wallis evaluation was also was utilised to determine differences in the sizes of the inhibitory zones produced by the CeO_2 NPs against each bacterial specimen.

Results and Discussion

Absorption spectroscopy

Fig. 2 demonstrates the absorption spectra of the green CeO_2 NPs synthesised in the present study. The maximum absorption band observed at 217 nm

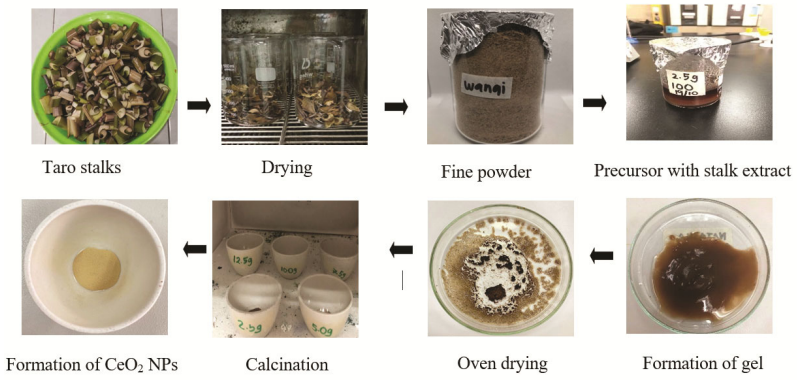

Fig. 1 — Biosynthesis of CeO_2 NPs using *C. esculenta* stalk extract

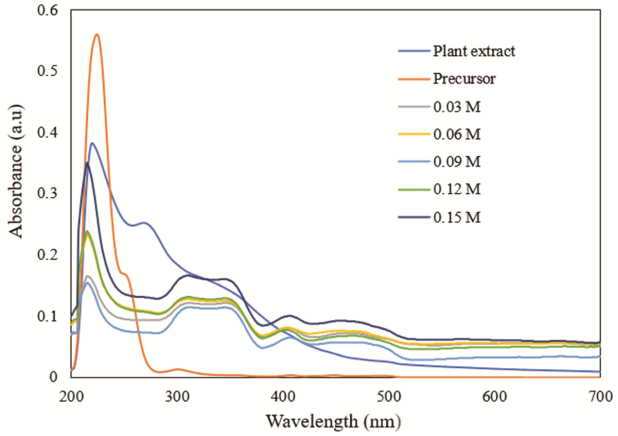

Fig. 2 — UV-visible absorption spectra of CeO_2 NPs in various concentration of precursor

Table 1 — Percentage yield (%) of the synthesised CeO_2 NPs at different concentration of precursor

Concentration of precursor (M)	Sample 1	Sample 2	Sample 3	Average
0.03	3.97	1.96	5.18	3.71
0.06	1.26	1.36	2.82	1.82
0.09	1.49	1.49	2.18	1.72
0.12	1.13	1.21	1.64	1.33
0.15	0.76	0.86	0.88	0.83

indicated the formation of CeO_2 NPs. Oxidising polyphenols, which were denoted by an expansion band, were crucial for preventing CeO_2 NPs aggregation[27]. Similar absorption bands were recorded by several studies that reported the synthesis of CeO_2 NPs with different plants.

Sathiyapriya *et al.*[28] reported that CeO_2 NPs derived from *Coriandrum sativum* L. leaf extract recorded a 276 nm absorption band, indicating successful synthesis of the NPs. The results were slightly similar to earlier studies on CeO_2 NPs synthesis utilising wet chemistry[29], which noted the presence of CeO_2 NPs at 253 nm. Jan *et al.*[30] also reported a significant absorption band at 298 nm, which indicated CeO_2 NPs development. In another study, Younas *et al.*[31] recorded a notable absorption peak (max) at 280 nm in the UV-Vis spectrum, reflecting the presence of CeO_2 NPs synthesised through the precipitation method. In the present study, the highest percentage yield was observed when the 0.03 M precursor was used (Table 1). Tesfaye *et al.*[32] emphasised that factors such as precursor concentration and the ratio of plant extract significantly influenced the yield, size, shape and uniformity of NPs. Manimaran *et al.*[33] also explored optimization techniques for green CeO_2 NPs

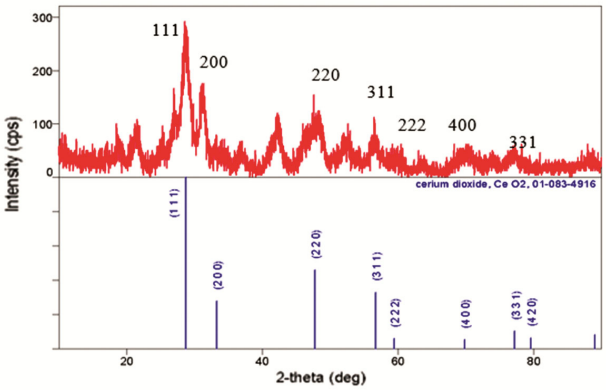

Fig. 3 — XRD pattern of CeO_2 NPs

synthesis, using a precursor concentration of 0.1, 0.2, 0.3, and 0.5 per 10 mL in *Azadirachta indica* leaf extract. In their study, the highest yield (15.43%) was obtained using optimised input parameters of 0.3 g/10 mL precursor concentration and 5 mL of *Azadirachta indica* leaf extract, centrifuged for 20 min. This highlights the critical role of precursor concentration as one of the optimization variable in the synthesis of CeO_2 NPs.

X-ray diffraction studies

Fig. 3 shows the XRD patterns of the biosynthesised CeO_2 NPs. The crystallographic arrangements of the CeO_2 NPs documented prominent diffraction peaks at 33.41°, 36.89°, 48.07°, 52.54°, 56.59°, 70.50°, and 77.23° (2θ), which corresponded to (111), (200), (220), (311), (222) (400), (331), and (420) lattice planes, respectively. The findings confirmed the crystalline nature of the CeO_2 NPs and aligned with the data reported by Zamani *et al.*[34]. Maqbool *et al.*[19] also recorded similar results for the CeO_2 NPs synthesised using *Olea europaea* leaf extract.

According to Debye-Scherrer's formula ($D=0.89\lambda/\beta \cos\theta$), the average crystallite size of the synthesised NPs were found to be 6.44 nm, which was smaller than the CeO_2 NPs produced with leaf extracts from other plants. For instance, the CeO_2 NPs synthesised utilising *Cassia angustifolia* was 36 nm[35]. In another report, Hkiri *et al.*[36] noted that the CeO_2 NPs produced with *Portulaca oleracea* had crystallites of approximately 16 nm.

TEM analysis

The average size and the morphology of the synthesised CeO_2 NPs were determined through TEM analysis. Fig. 4(a) and (b) demonstrate the morphological characteristics of the biosynthesised

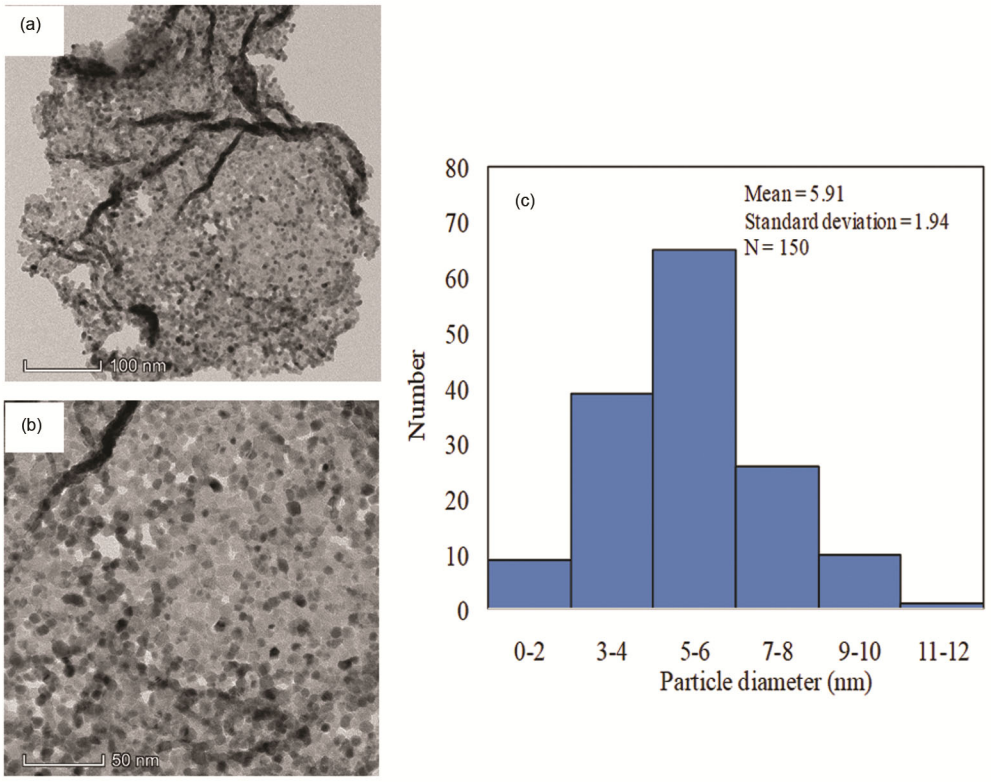

Fig. 4 — (a & b) TEM images at different magnifications and (c) corresponding histogram of CeO_2 NPs

CeO_2 NPs at different magnifications. Based on the results, most of the particles were nearly spherical. Khatami *et al.*[37] reported a similar spherical structure of the CeO_2 NPs synthesised utilising *Stevia rebaudiana* sugar leaf extract. Arunachalam *et al.*[18] also observed spherical CeO_2 NPs derived from *Prosopis juliflora* mesquite leaf extract.

Fig. 4(c) illustrates the histogram of 150 randomly selected CeO_2 NPs distribution. The particles were analysed with ImageJ software. On average, the CeO_2 NPs was found to be 5.91 nm. The data was consistent with the figures obtained with Scherrer's formula.

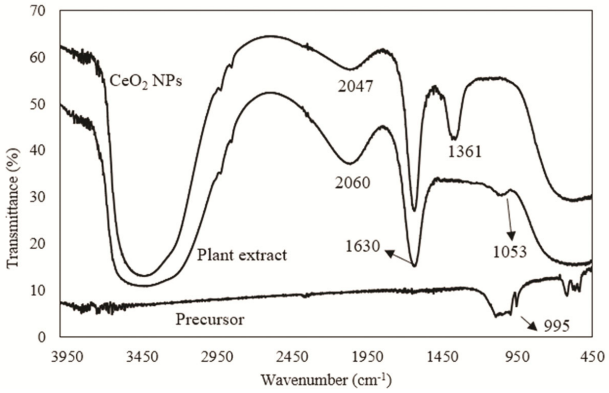

Fig. 5 — FTIR analysis of CeO_2 NPs, plant extract and precursor

FTIR analysis

The present study conducted FTIR studies to ascertain the involvement of bioactive chemicals in *C. esculenta* stalk extract in the formation of the CeO_2 NPs. The FTIR spectrum (Fig. 5) demonstrated notable absorption peaks within the 4000–500 cm^{-1} wavenumber range. The spectral region from 2500 cm^{-1} to approximately 4,000 cm^{-1} corresponds to O–H and C–H stretching[38,39]. Consequently, the extensive absorption observed within the 3750–3000 cm^{-1} frequency range could be attributed to the stretching vibrations of O–H bonds resulting from residual alcohol, water, and Ce–OH groups. The functional groups in the *C. esculenta* stalk extract produced peaks at 1630 cm^{-1} and 2047 cm^{-1}, which were associated to C=C from its phytochemical components. Similar were recorded by the CeO_2 NPs synthesised, indicating the presence of the plant extract that reduced the Ce(IV) ion to Ce metal and stabilised the resultant NPs[40]. Prominent peaks observed at 3400 cm^{-1} and 1600 cm^{-1} also aligned with the findings reported by Kumar *et al.*[41]. The study utilised petals derived from the Cinnamon-like

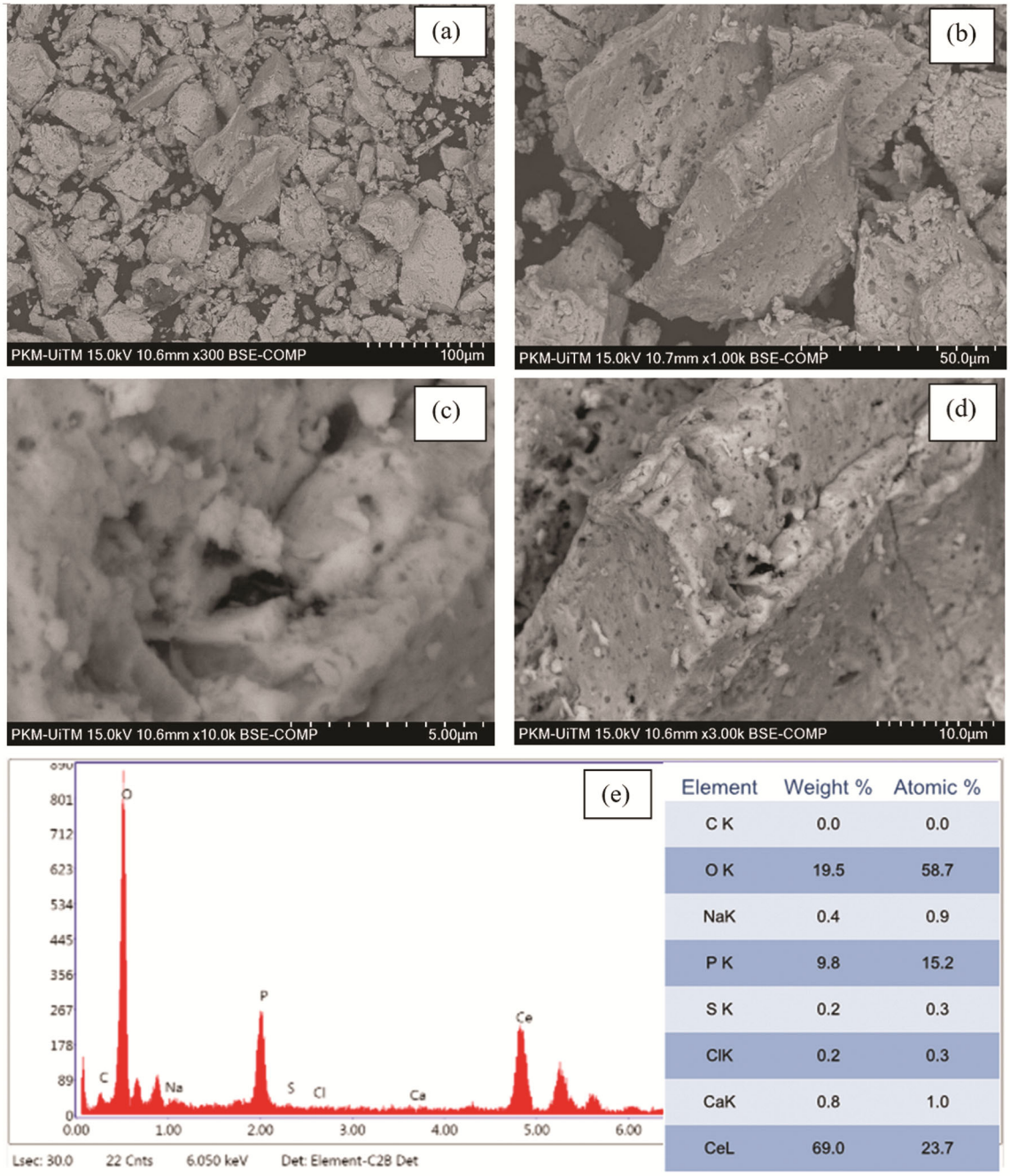

Element	Weight %	Atomic %
C K	0.0	0.0
O K	19.5	58.7
NaK	0.4	0.9
P K	9.8	15.2
S K	0.2	0.3
ClK	0.2	0.3
CaK	0.8	1.0
CeL	69.0	23.7

Fig. 6 — SEM of CeO_2 NPs at (a) 100 µm, (b), 50 µm, (c) 10 µm, (d) 5 µm and (e) EDX analysis

bark of *Cassia glauca* as the capping agent during synthesis of CeO_2 NPs.

SEM and EDX analysis

Fig. 6 illustrates the SEM mocrographs of CeO_2 NPs at different magnifications. Based on Figs 6(a)–(d), the CeO_2 NPs had irregular shapes with slight agglomeration. The non-uniform shape of the CeO_2 NPs was comparable to the report by Alam *et al.*[24]. Yadav *et al.*[35] synthesised CeO_2 NPs utilising fruit juice extract and documented agglomeration. van der Waals adhesion forces between the various non-magnetic CeO_2 NPs might led to the agglomeration[42].

The EDX spectrum (Fig. 6e) showed high-intensity peaks of Ce (69.0%) and O (19.5%) and several impurities, such as phosphorus, calcium, sodium, and

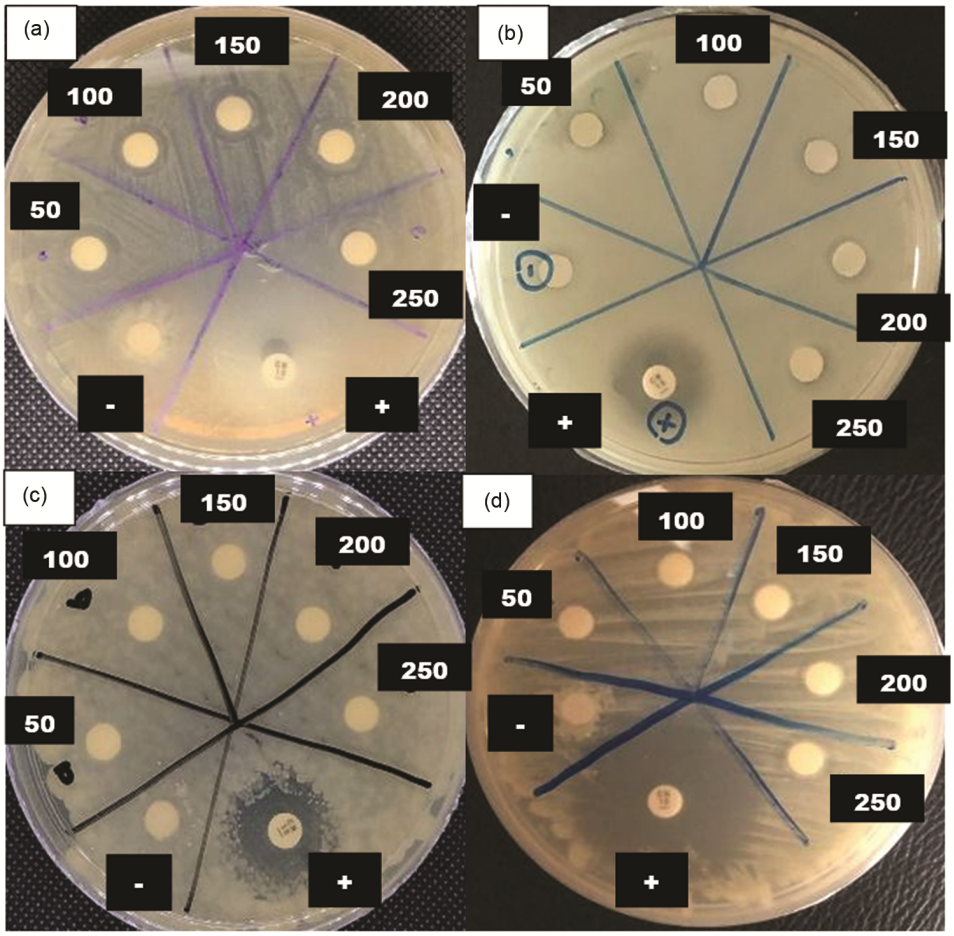

Fig. 7 — Inhibition zone of synthesized CeO_2NPs against some bacteria (a) *E.coli*, (b) *K.pneumoniae*, (c) *B.subtilis* and (d) *S.aureus*

chlorine. Farahmandjou *et al.*[43] also detected impurities in the CeO_2 NPs procured. The report noted Cl (0.61%), nitrogen (21.69%), P (6.57%), and potassium (6.57%) in the NPs. Thovhogi *et al.*[20] reported similar findings and suggested that the impurities were due to the natural organic compounds in the plant extracts employed.

Antibacterial activity

Disc-diffusion assay offers several advantages compared to other techniques, including simplicity, affordability, flexibility, and ease of data interpretation[44]. Consequently, the approach is widely employed in antibacterial activity evaluations of engineered nanomaterials in laboratory settings and complex matrices[45]. The antimicrobial properties of the CeO_2 NPs against Gram-positive and Gram - negative bacterial cultures were determined via the disc diffusion method and the results are shown in Fig. 7.

Although the CeO_2 NPs had adverse effect on all bacterial strains evaluated, *B. subtilis* is found to be more resistance to the NPs. All bacterial cultures also exhibited susceptibility across CeO_2 NPs concentrations (50–250 µg/mL). Nonetheless, interactions between the NPs and the bacteria varied[46]. Qi *et al.*[47] suggested that CeO_2 NPs exhibited superior efficacy against Gram-negative bacteria (*E. coli*) than Gram-positive bacteria (*B. subtilis*), as evidenced by a slight decrease in viability. The findings were also supported by the report of Sang *et al.*[48], which reported good inhibition activities of the Ce complex against *B. subtilis*.

Bacterial cell wall structures are critical in effectiveness against antibacterial activities. Gram-positive bacteria possess denser and thicker cell walls than their Gram-negative counterparts. Consequently, the microorganisms are more protected and less affected than Gram-negative bacteria by the CeO_2 NPs. Conversely, Gram-negative bacteria have thinner cell walls, hence more vulnerable to antimicrobial effects than their Gram-positive counterparts[49].

Table 2 — Antibacterial activity of biosynthesized CeO_2 NPs against pathogenic bacteria

Bacteria	Positive control (gentamicin 10 µg)	Diameter of inhibition zone (mm) of different concentration of CeO_2 NPs (mean ± SD)					Negative control
		50 µg/mL	100 µg/mL	150 µg/mL	200 µg/mL	250 µg/mL	
Klebsiella pneumonia [ab]	20±1.0	4.7±0.6	5.7± 0.6	6.0±1.0	8.7±0.6	8.3 ±1.2	-
Escherichia coli [ab]	19±1.0	10.7±1.2	13±1.0	12.3±2.1	10.3 ±0.6	10.3±0.6	-
Staphylococcus aureus[ab]	31±5.9	3. ±1.2	3.7±0.6	7.0±1.0	6.7±1.2	13.3±0.6	-
Bacillus subtilis [a]	18±1.0	-	-	-	-	-	-

Note: - indicated no inhibition zone

Values are represented as mean ± SD

Variable with the different letter within column are significantly different at $p<0.05$, according to pairwise test

Ayodhya *et al.*[50] investigated the antimicrobial properties of CeO_2 NPs synthesised utilising Sapodilla fruit (*Manilkara zapota*) peel waste. The study found that *E. coli* was susceptible to the NPs, whereas *S. aureus* and *B. subtilis* were less affected due to their distinctive cell wall structure. Furthermore, electrostatic variations between the NPs manufactured in the study aided its resistance to antimicrobial treatments.

In this study, the effects of varying CeO_2 NPs concentrations(50–250 µg/mL) against the bacterial cultures were established (Table 2 and Fig. 7). The disc diffusion results documented improved inhibition zones against *E.coli* and *S.aureus* when the concentration of the NPs utilised was increased between 50 and 150 ug/mL. Roudbaneh *et al*.[51] also reported similar findings.

The CeO_2 NPs at concentrations from 100 to 150 µg/mL exhibited the largest inhibition zone (10 mm) against *S.aureus*. The microorganism was also the most susceptible bacteria towards the NPs in the Gram-positive bacteria group assessed. The antibacterial activities of CeO_2 NPs against *S. aureus* were also established by Malleshappa *et al*.[52]. In the Gram-negative category, the CeO_2 NPs synthesised in this study produced the most significant inhibition zone against *E. coli* when employed at 100 µg/mL. *S.aureus* was the most affected by the CeO_2 NPs, recording maximum inhibition at 250 µg/mL of the NPs. Distinct inhibition diameters of 13 mm against *E.coli* and 13.3 mm against *S.aureus* were documented when different doses of the CeO_2 NPs were utilised. Nevertheless, no significant differences between varying CeO_2 NPs concentrations against the microorganisms were established when analysed with Kruskal-Wallis. Statistical analysis utilising Spearman's Rho indicated non-significant correlations between the inhibition zone diameters and the bacterial strains. Furthermore, the CeO_2 NPs manufactured in the current study exhibited a weak association value across all bacteria assessed ($r= -0.150$) and inhibition zones (0.109). The negative or inverse link indicated that concentration increments lead to decreased bacterial inhibition zone diameter.

Conclusion

The current study highlighted the potential of *C. esculenta* stalk extract playing a dual-role i.e., as reducing and capping agents, during the synthesis of CeO_2 NPs. Successful NPs formation was evidenced by the absorption peak at 219 nm in the UV-visible absorption results. The average crystallite size was calculated to be 6.44 nm using Scherrer equation. XRD data aligned with the TEM images (5.91 nm), further affirming the efficacy of the synthesis method. The NPs also exhibited nearly spherical morphology, indicating precise control over particle formation with the employment of the *C. esculenta* stalk extract. Although the CeO_2 NPs demonstrated significant antibacterial activities, the nanomaterial exhibited notable resilience against *B. subtilis*. The straightforward and one-step synthesis procedure proposed in the current study offers a cost-effective, simple, safe, and appealing alternative to conventional chemical techniques.

Acknowledgements

The authors extend their sincere gratitude to the Malaysian Ministry of Higher Education for funding this study through the Fundamental Research Grant Scheme (Grant No. FRGS-RMC 600 5/3 056/2022). Appreciation is also given to Universiti Teknologi

MARA for providing the necessary facilities and to the Malaysian Agricultural Research and Development Institute (MARDI) for supplying the Taro stalks.

References

1 Eka-Putri G, Rilda Y, Syukri S, Labanni A & Arief S, Highly antimicrobial activity of cerium oxide nanoparticles synthesized using Moringa oleifera leaf extract by a rapid green precipitation method, *J Mater Res Technol*, 15 (2021) 2355.

2 Wasef L, Nassar A M K, El-Sayed Y S, Samak D, Noreldin A, Elshony N, Saleh H, Elewa Y H A, Hassan S M A, Saati A A, Hetta H F, Batiha G E S, Umezawa M & Shaheen H M, The potential ameliorative impacts of cerium oxide nanoparticles against fipronil-induced hepatic steatosis, *Sci Rep*, 11 (2021) 1.

3 Lu L, Dai G, Yan L, Wang L, Wang L, Wang Z & Wei K, In-situ low-temperature sol-gel growth of nano-cerium oxide ternary composite films for ultraviolet blocking, *Opt Mater*, 101 (2020) 1.

4 Kusuma K B, Manju M, Ravikumar C R, Raghavendra N, Amulya M A S, Nagaswarupa H P, Murthy H C A, Kumar M R A & Shekhar T R S, Photocatalytic degradation of Methylene Blue and electrochemical sensing of paracetamol using Cerium oxide nanoparticles synthesized via sonochemical route, *Appl Surf Sci Adv*, 11 (2022) 1.

5 Ramachandran M, Subadevi R & Sivakumar M, Role of pH on synthesis and characterization of cerium oxide (CeO_2) nano particles by modified co-precipitation method, *Vacuum*, 161 (2019) 220.

6 Trenque I, Magnano G C, Bárta J, Chaput F, M A Bolzinger, Pitault I, Briançon S, Masenelli-Varlot K, Bugnet M, Dujardin C, Čuba V & Amans D, Exposure, synthesis routes of CeO_2 nanoparticles dedicated to organophos-phorus degradation: A benchmark, *Cryst Eng Comm*, 22 (2020) 1725.

7 Barman K, Dutta P, Chowdhury D & Baruah P K, Green biosynthesis of copper oxide nanoparticles using waste colocasia esculenta leaves extract and their application as recyclable catalyst towards the synthesis of 1,2,3-triazoles, *Bionanoscience*, 11 (2021) 189.

8 Paiva-Santos A C, Herdade A M, Guerra C, Peixoto D, Pereira-Silva M, Zeinali M, Mascarenhas-Melo F, Paranhos A & Veiga F, Plant-mediated green synthesis of metal-based nanoparticles for dermopharmaceutical and cosmetic applications, *Int J Pharm*, 597 (2021) 1.

9 Garg D, Sarkar A, Chand P, Bansal P, Gola D, Sharma S, Khantwal S, Mehrotra S R, Chauhan N & Bharti R K, Synthesis of silver nanoparticles utilizing various biological systems: Mechanisms and applications-A review, *Prog Biomater*, 9 (2020) 81.

10 Radulescu D M, Surdu V A, Ficai A, Ficai D, Grumezescu A M & Andronescu E, Green synthesis of metal and metal oxide nanoparticles: A review of the principles and biomedical applications, *Int J Mol Sci*, 24 (2023) 1.

11 Moosavy M H, Dela-Guardia M, Mokhtarzadeh A, Khatibi S A, Hosseinzadeh N & Hajipour N, Green synthesis, characterization, and biological evaluation of gold and silver nanoparticles using Mentha spicata essential oil, *Sci Rep*, 13 (2023) 1.

12 Barabadi H, Mojab F, Vahidi H, Marashi B, Talank N, Hosseini O & Saravanan M, Green synthesis, characterization, antibacterial and biofilm inhibitory activity of silver nanoparticles compared to commercial silver nanoparticles, *Inorg Chem Commun*, 129 (2021) 1.

13 Singh H, Desimone M F, Pandya S, Jasani S, George N, Adnan M, Aldarhami A, Bazaid A S & Alderhami S A, Revisiting the green synthesis of nanoparticles: Uncovering influences of plant extracts as reducing agents for enhanced synthesis efficiency and its biomedical applications, *Int J Nanomed*, 18 (2023) 4727.

14 Ovais M, Khalil A T, Islam N U, Ahmad I, Ayaz M, Saravanan M, Shinwari Z K & Mukherjee S, Role of plant phytochemicals and microbial enzymes in biosynthesis of metallic nanoparticles, *Appl Microbiol Biotechnol*, 102 (2018) 6799.

15 Arumugam A, Karthikeyan C, Haja H A S, Gopinath K, Gowri S & Karthika V, Synthesis of cerium oxide nanoparticles using Gloriosa superba L. leaf extract and their structural, optical and antibacterial properties, *Mater Sci Eng C*, 49 (2015) 408.

16 Kannan S K & Sundrarajan M, A green approach for the synthesis of a cerium oxide nanoparticle: Characterization and antibacterial activity, *Int J Nanosci*, 13 (2014) 1.

17 Sebastiammal S, Sonia S, Henry J & Lesly F A, Green synthesis of cerium oxide nanoparticles using aloevera leaf extract and its optical properties, *Songklanakarin J Sci Technol*, 43 (2021) 582.

18 Arunachalam T, Karpagasundaram U & Rajarathinam N, Ultrasound assisted green synthesis of cerium oxide nanoparticles using Prosopis juliflora leaf extract and their structural, optical and antibacterial properties, *Mater Sci Pol*, 35 (2017) 791.

19 Maqbool Q, Nazar M, Naz S, Hussain T, Jabeen N, Kausar R, Anwaar S, Abbas F & Jan T, Antimicrobial potential of green synthesized CeO_2 nanoparticles from Olea europaea leaf extract, *Int J Nanomed*, 11 (2016) 5015.

20 Thovhogi N, Diallo A, Gurib-Fakim A & Maaza M, Nanoparticles green synthesis by Hibiscus Sabdariffa flower extract: Main physical properties, *J Alloys Compd*, 647 (2015) 392.

21 Muthuvel A, Jothibas M, Mohana V & Manoharan C, Green synthesis of cerium oxide nanoparticles using Calotropis procera flower extract and their photocatalytic degradation and antibacterial activity, *Inorg Chem Commun*, 119 (2020) 1.

22 Kalaskar M, Rajput R & Tatiya A, Physicochemical and phytochemical analysis of colocasia esculenta: A promising nutritional food plant, *Int J Adv Res Biol Sci*, 10 (2023) 8.

23 Mondal A, Hajra A, Shaikh W, Chakraborty S & Mondal N, Synthesis of silver nanoparticle with Colocasia esculenta (L.) stem and its larvicidal activity against Culex quinquefasciatus and Chironomus sp, *Asian Pac J Trop Biomed*, 9 (2019) 510.

24 Alam M W, Naeem S, Usman S M, Kanwal Q, Ba-Qais A, Aldughaylibi F S, Nahvi I & Zaidi N, Cerium oxide nanorods synthesized by Dalbergia sissoo extract for antioxidant, cytotoxicity, and photocatalytic applications, *Molecules*, 27 (2022) 1.

25 Ahmad N M & Hasan N, Synthesis of green cerium oxide nanoparticles using plant waste from colocasia esculenta for seed germination of mung bean (Vigna radiata), *J Nanotechnol*, 2023 (2023) 1.

26 Dar M A, Gul R, Karuppiah P, Al-Dhabi N A & Alfadda A A, Antibacterial activity of cerium oxide nanoparticles against ESKAPE pathogens, *Crystals*, 12 (2022) 1.

27 Ahmed H E, Iqbal Y, Aziz M H, Atif M, Batool Z, Hanif A, Yaqub N, Farooq W A, Ahmad S, Fatehmulla A & Ahmad H, Green synthesis of CeO_2 nanoparticles from the abelmoschus esculentus extract: Evaluation of antioxidant, anticancer, antibacterial, and wound-healing activities, *Molecules*, 26 (2021) 1.

28 Sathiyapriya R, Balaji M & Rajesh S, Bio-synthesis of cerium oxide nanoparticles from coriandrum sativum L. leaf extract and their antibacterial activity, *Int J Adv Sci Eng*, 6 (2020) 1439.

29 Estes L M, Singha P, Singh S, Sakthivel T S, Garren M, Devine R, Brisbois E J, Seal S & Handa H, Characterization of a nitric oxide (NO) donor molecule and cerium oxide nanoparticle (CNP) interactions and their synergistic antimicrobial potential for biomedical applications, *J Colloid Interface Sci*, 586 (2020) 163.

30 Jan H, Khan M A, Usman H, Shah M, Ansir R, Faisal S, Ullah N & Rahman L, The Aquilegia pubiflora(Himalayan columbine) mediated synthesis of nanoceria for diverse biomedical applications, *RSC Adv*, 10 (2020) 19219.

31 Younas M, Zubair M, Rizwan M, Khan M A, Hussaini K M, Mumtaz R, Azeem M, Abbas T, Irshad M A & Ali S, Synthesis and characterization of cerium, silver and copper oxide nanoparticles and their anticancer potential of hepatocellular carcinoma $HepG_2$ cancer cells, *J Mol Struct*, 1288 (2023) 1.

32 Tesfaye M, Gonfa Y, Tadesse G, Temesgen T & Periyasamy S, Green synthesis of silver nanoparticles using Vernonia amygdalina plant extract and its antimicrobial activities, *Heliyon*, 9 (2023) 1.

33 Manimaran R, Optimization of Azadirachta indica leaf extract mediated cerium oxide nanoparticles synthesis, characterization, and its applications, *Ind Crops Prod*, 204 (2023) 1.

34 Zamani A & Marjani A P, Walnut shell-templated ceria nanoparticles: Green synthesis, characterization and catalytic application, *Int J Nanosci*, 17 (2018) 1.

35 Yadav L S R, Manjunath K, Archana B, Madhu C, Naika H R, Nagabhushana H, Kavitha C & Nagaraju G, Fruit juice extract mediated synthesis of CeO_2 nanoparticles for antibacterial and photocatalytic activities, *Eur Phys J Plus*, 131 (2016) 1.

36 Hkiri K, Ahmed M H E, Ghotekar S & Maaza M, Green synthesis of cerium oxide nanoparticles using Portulaca oleracea extract: Photocatalytic activities, *Inorg Chem Commun*, 162 (2024) 1.

37 Khatami M, Sarani M, Mosazadeh F, Rajabalipour M, Izadi A, Abdollahpour-Alitappeh M, Nobre M A L & Borhani F, Nickel-doped cerium oxide nanoparticles: Green synthesis using stevia and protective effect against harmful ultraviolet rays, *Molecules*, 24 (2019) 1.

38 Phoka S, Laokul P, Swatsitang E, Promarak V, Seraphin S & Maensiri S, Synthesis, structural and optical properties of CeO_2 nanoparticles synthesized by a simple polyvinyl pyrrolidone (PVP) solution route, *Mater Chem Phys*, 115 (2009) 423.

39 Calvache-Muñoz J, Prado F A & Rodríguez-Páez J E, Cerium oxide nanoparticles: Synthesis, characterization and tentative mechanism of particle formation, *Colloids Surf A Physicochem Eng Asp*, 529 (2017) 146.

40 Dutta D, Mukherjee R, Patra M, Banik M, Dasgupta R, Mukherjee M & Basu T, Green synthesized cerium oxide nanoparticle: A prospective drug against oxidative harm, *Colloids Surfaces B Biointerfaces*, 147 (2016) 45.

41 Kumar E, Selvarajan P & Balasubramanian K, Preparation and studies of cerium dioxide(CeO_2) nanoparticles by microwave-assisted solution method, *Recent Res Sci Technol*, 2 (2010) 37.

42 Alexander P S, Ramachandran B & Chandrasekar N, Green synthesis of cerium nanoparticles using hibiscus rosasinesis extract and evaluation of their antimicrobial activity and photocatalytic activity, *Mater Today Proc*, 90 (2023) 30.

43 Farahmandjou M, Zarinkamar M & Firoozabadi T P, Synthesis of cerium oxide (CeO_2) nanoparticles using simple Co-precipitation method, *Rev Mex Física*, 62 (2016) 496.

44 Balouiri M, Sadiki M & Ibnsouda S K, Methods for in vitro evaluating antimicrobial activity: A review, *J Pharm Anal*, 6 (2016) 71.

45 Zhang X, Hou X, Ma L, Shi Y, Zhang D & Qu K, Analytical methods for assessing antimicrobial activity of nanomaterials in complex media: Advances, challenges, and perspectives, *J Nanobiotechnol*, 21 (2023) 1.

46 Pelletier D A, Suresh A K, Holton G A, McKeown C K, Wang W, Gu B, Mortensen N P, Allison D P, Joy D C, Allison M R, Brown S D, Phelps T J & Doktycz M J, Effects of engineered cerium oxide nanoparticles on bacterial growth and viability, *Appl Environ Microbiol*, 76 (2010) 7981.

47 Qi M, Li W, Zheng X, Li X, Sun Y, Wang Y, Li C & Wang L, Cerium and its oxidant-based nanomaterials for antibacterial applications: A state-of-the-art review, *Front Mater*, 7 (2020) 1.

48 Sang Y L, Lin X S, Li X C, Liu Y H & Zhang X H, Synthesis, crystal structure and antibacterial activity of a novel phenolato- and peroxo-bridged dinuclear cerium(IV) complex with tripodal Schiff bases, *Inorg Chem Commun*, 62 (2015) 115.

49 Pop O L, Mesaros A, Vodnar D C, Suharoschi R, Tăbăran F, Mageruşan L, Tódor I S, Diaconeasa Z, Balint A, Ciontea L & Socaciu C, Cerium oxide nanoparticles and their efficient antibacterial application in vitro against gram-positive and gram-negative pathogens, *Nanomaterials*, 10 (2020) 1.

50 Ayodhya D, Ambala A, Balraj G, Kumar M P & Shyam P, Green synthesis of CeO_2 NPs using Manilkara zapota fruit peel extract for photocatalytic treatment of pollutants, antimicrobial, and antidiabetic activities, *Results Chem*, 4 (2022) 1.

51 Roudbaneh S Z K, Kahbasi S, Sohrabi M J, Hasan A, Salihi A, Mirzaie A, Niyazmand A, Nanakali N M Q, Shekha M S, Aziz F M, Vaghar-Lahijani G, Keshtali A B, Ehsani E, Rasti B & Falahati M, Albumin binding, antioxidant and antibacterial effects of cerium oxide nanoparticles, *J Mol Liq*, 296 (2019) 1.

52 Malleshappa J, Nagabhushana H, Sharma S C, Vidya Y S, Anantharaju K S, Prashantha S C, Prasad B D, Naika H R, Lingaraju K & Surendra B S, Leucas aspera mediated multi-functional CeO_2 nanoparticles: Structural, photoluminescent, photocatalytic and antibacterial properties, *Spectrochim Acta-Part A Mol Biomol Spectrosc*, 149 (2015) 452.